RAGTIME
27TH RELATIVISTIC ASTROPHYSICS GROUP MEETING
November 10th - 14th 2025

SILESIAN UNIVERSITY IN OPAVA

Magnetic vs. Relativistic Disk Precession Models for QPOs in PULX Sources

Sukalpa Kundu
Supervisors: Włodek Kluźniak, Miljenko Čemeljić

Work done at: CAMK PAN, Warsaw

CAMK PAN

Pulsating Ultraluminous X-Ray Sources

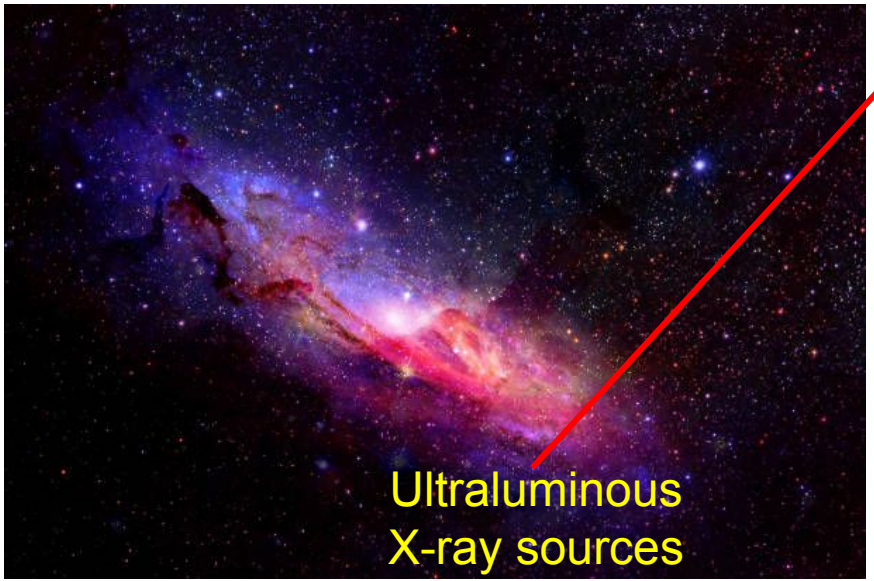

$$L_{\mathrm{X}} \approx 10^{39} - 10^{41} \mathrm{erg\ s^{-1}}$$

Pulsating Ultraluminous X-Ray Sources

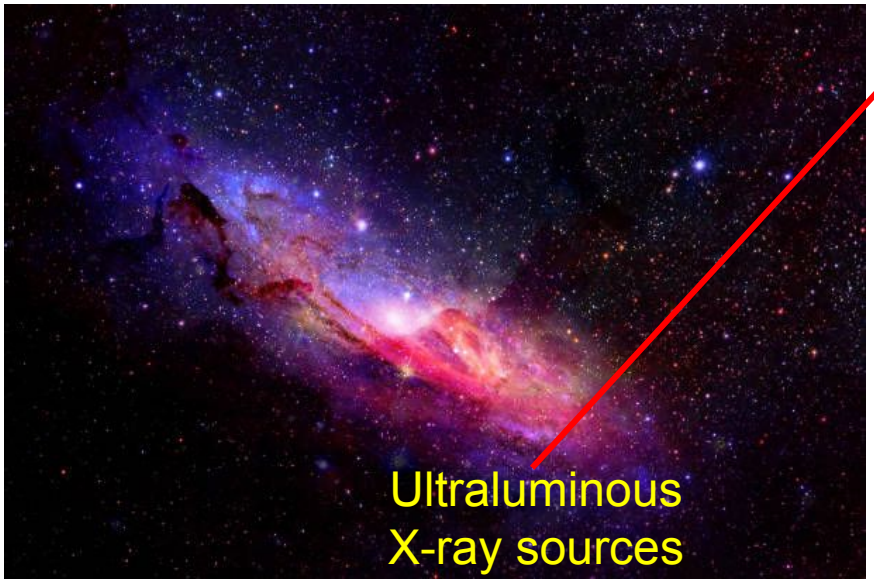

$$L_{\rm X} \approx 10^{39} - 10^{41} {\rm erg\ s^{-1}}$$

$$P_* \sim \mathcal{O}({\rm s})$$

Coherent pulsation (neutron stars)

Bachetti+14

Pulsating Ultraluminous X-Ray Sources

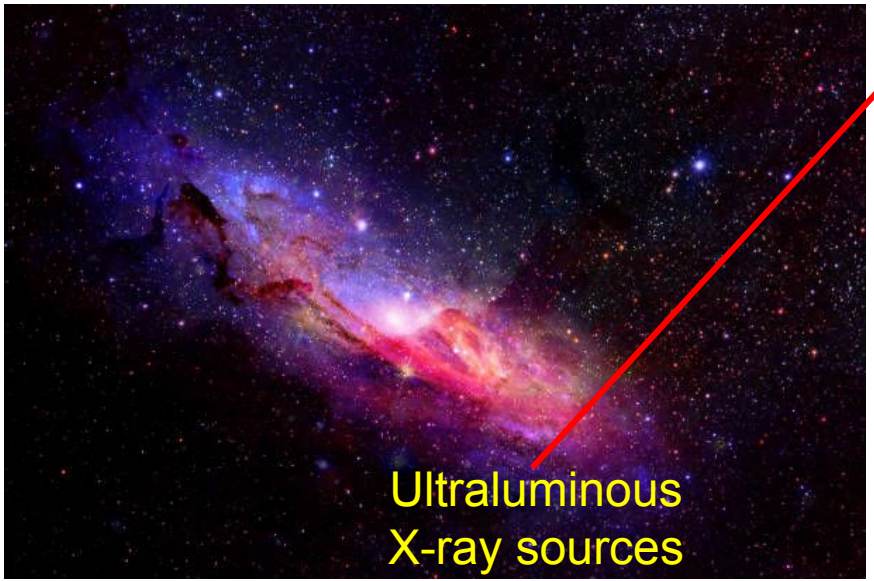

$$L_{\rm X} \approx 10^{39} - 10^{41} {\rm erg\ s^{-1}}$$

$$P_* \sim \mathcal{O}({\rm s})$$

Coherent pulsation (neutron stars)

Bachetti+14

Pulsating **U**l**t**ra**l**uminous **X**-Ray Sources (PULX)

Pulsating Ultraluminous X-Ray Sources

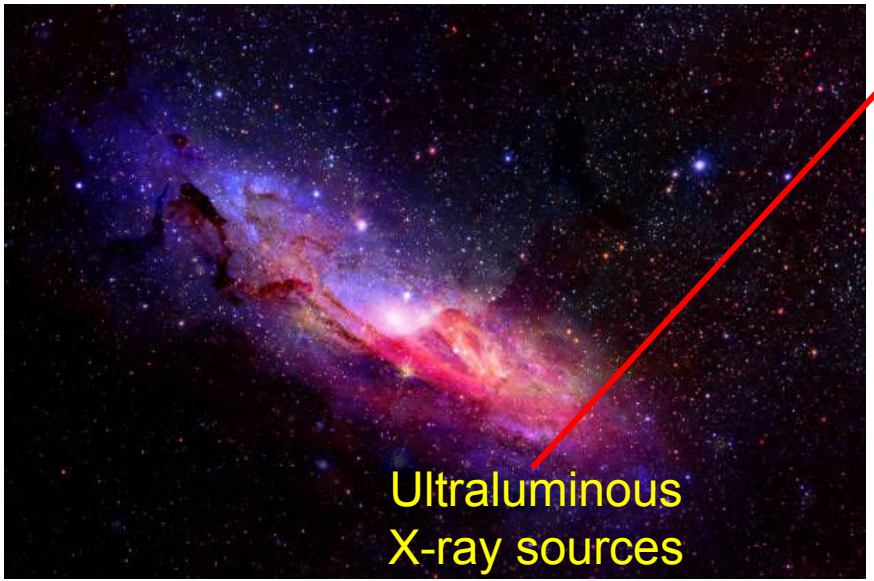

$$L_{\rm X} \approx 10^{39} - 10^{41} {\rm erg\ s^{-1}}$$

$$P_* \sim \mathcal{O}({\rm s})$$

Coherent pulsation (neutron stars)

Bachetti+14

Pulsating **U**l**t**ra**l**uminous **X**-Ray Sources (PULX)

$$L_{{\rm Edd},\odot} = 1.3 \times 10^{38} {\rm erg\ s^{-1}}$$

Luminosity much higher than Eddington luminosity for neutron stars

Magnetar vs Beaming

Magnetar Model:

$$L_{\rm Edd} \approx \frac{4\pi G M m_{\rm p} c}{\sigma_{\rm T}}$$

At B~10^{14}G, The free electron scattering opacity reduces sharply and increases the Eddington luminosity (Paczynski 92)

Magnetar vs Beaming

Magnetar Model:

$$L_{\rm Edd} \approx \frac{4\pi G M m_{\rm p} c}{\sigma_{\rm T}}$$

At B~10^{14}G, The free electron scattering opacity reduces sharply and increases the Eddington luminosity (Paczynski 92)

Beaming Model:

The emitted radiation is beamed instead of being isotropic.

$$L_{\rm obs} = L_{\rm Edd}/b$$

(King+01)

Quasi-Periodic Oscillations (QPOs)

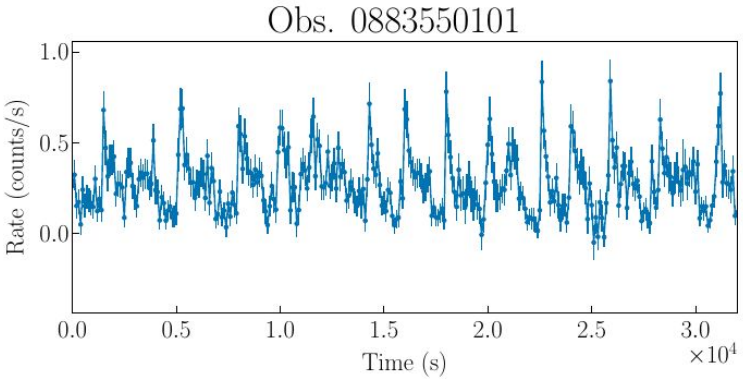

Figs from Imbrogno+24, ULX-7 M51

Quasi-Periodic Oscillations (QPOs)

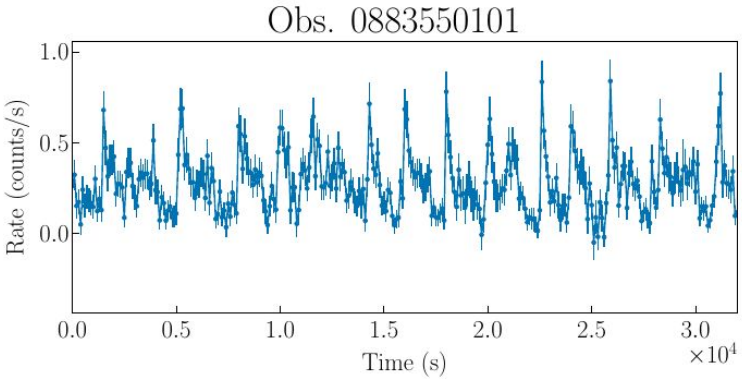

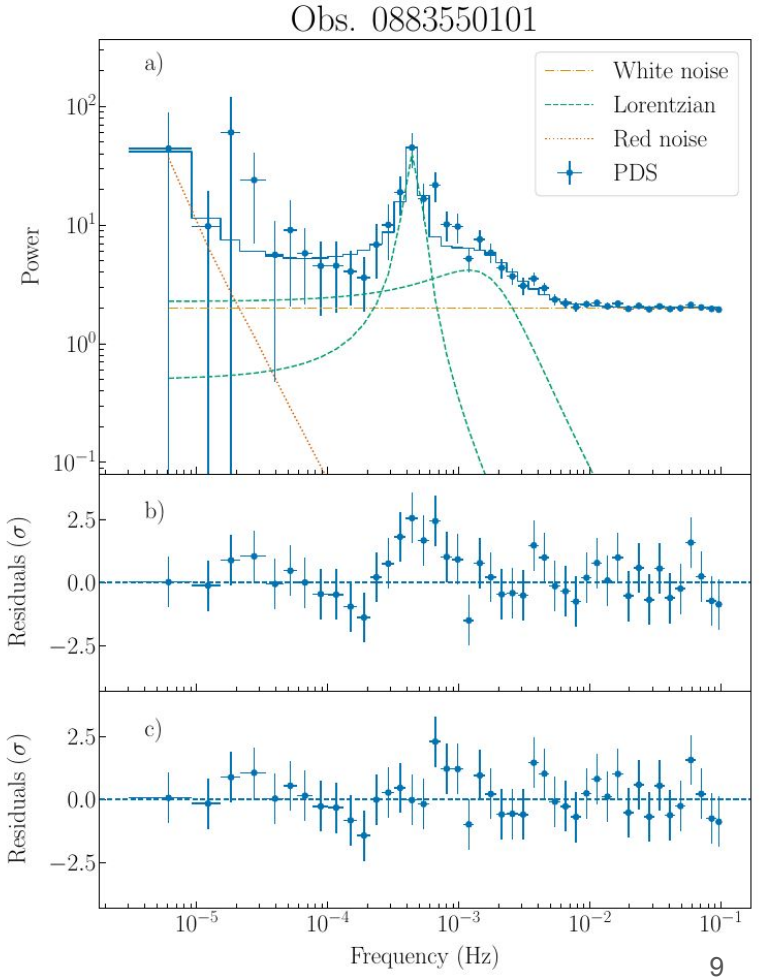

Figs from Imbrogno+24, ULX-7 M51

PULX mHz QPOs: The Problem

Fig from Čemeljić, Kluźniak, Kundu 25.

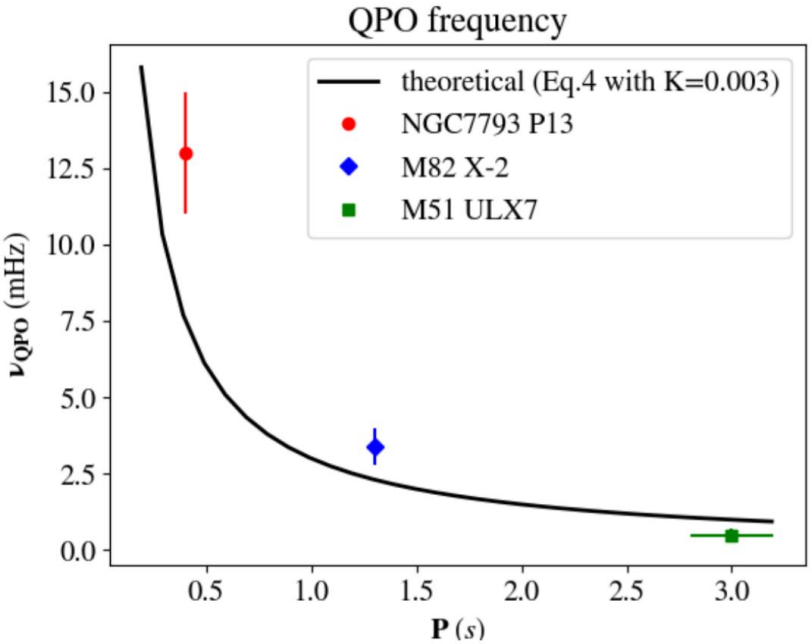

Till date, we have only three PULX sources that show QPOs in mHz range

PULX mHz QPOs: The Problem

Fig from Čemeljić, Kluźniak, Kundu 25.

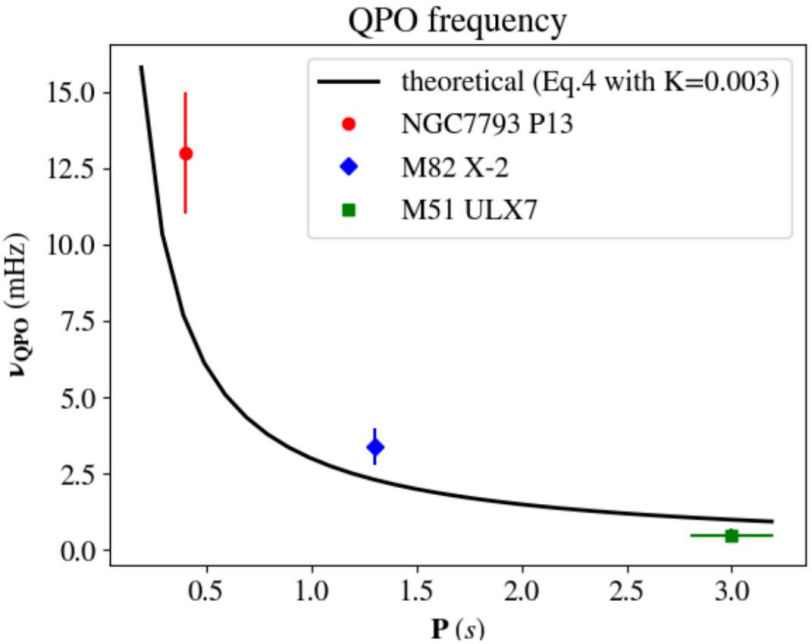

Till date, we have only three PULX sources that show QPOs in mHz range

Observation: QPO frequency and Spin Period are inversely related

(Čemeljić, Kluźniak, Kundu 25)

PULX mHz QPOs: The Problem

Fig from Čemeljić, Kluźniak, Kundu 25.

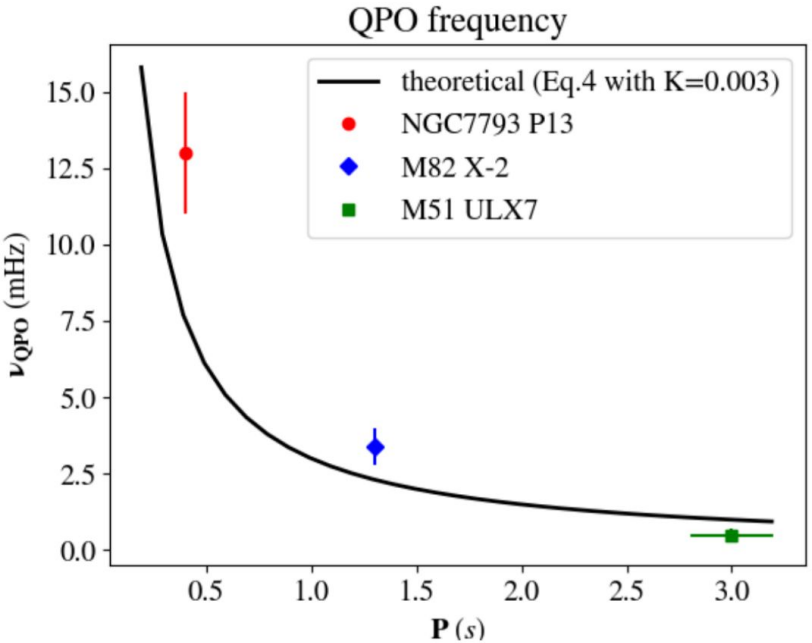

Till date, we have only three PULX sources that show QPOs in mHz range

Observation: QPO frequency and Spin Period are inversely related

(Čemeljić, Kluźniak, Kundu 25)

Possible Models: General Relativistic Precession vs Magnetic Precession

Case 1. The Lense-Thirring Precession

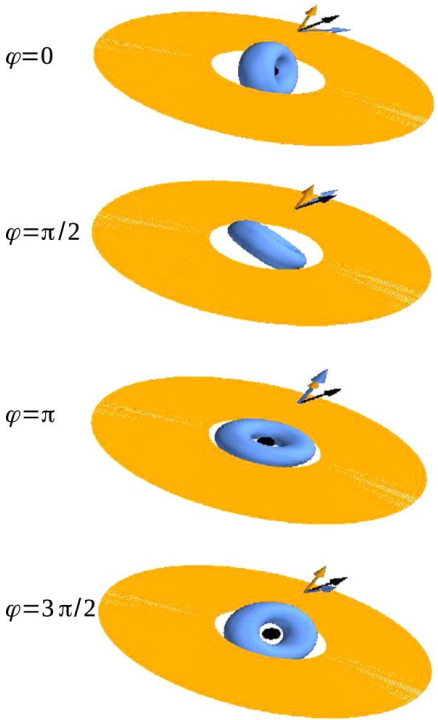

Fig from You+18

$$2\pi\nu_{\rm LT} = \frac{2a_* c r_{\rm g}^2}{r^3}$$

a_* : dimensionless spin parameter

$r_{\rm g}$: gravitational radius

Case 1. The Lense-Thirring Precession

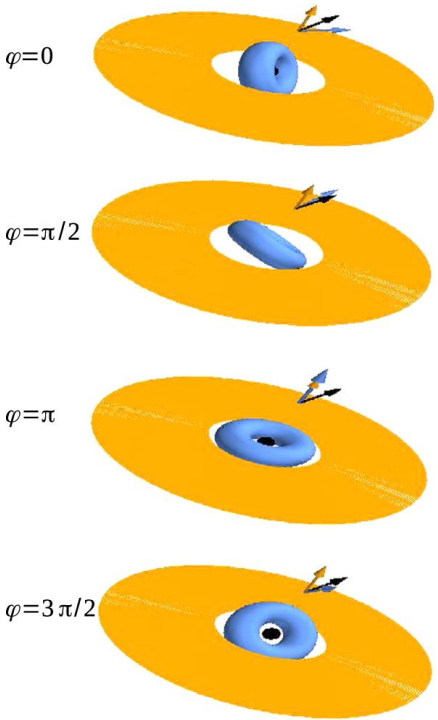

Fig from You+18

$$2\pi\nu_{\rm LT} = \frac{2a_* c r_{\rm g}^2}{r^3}$$

a_* : dimensionless spin parameter

$r_{\rm g}$: gravitational radius

QPO frequency, spin period from observation provides **radial distance (*r*)** of LT precession

The Constraint : Position of Magnetosphere

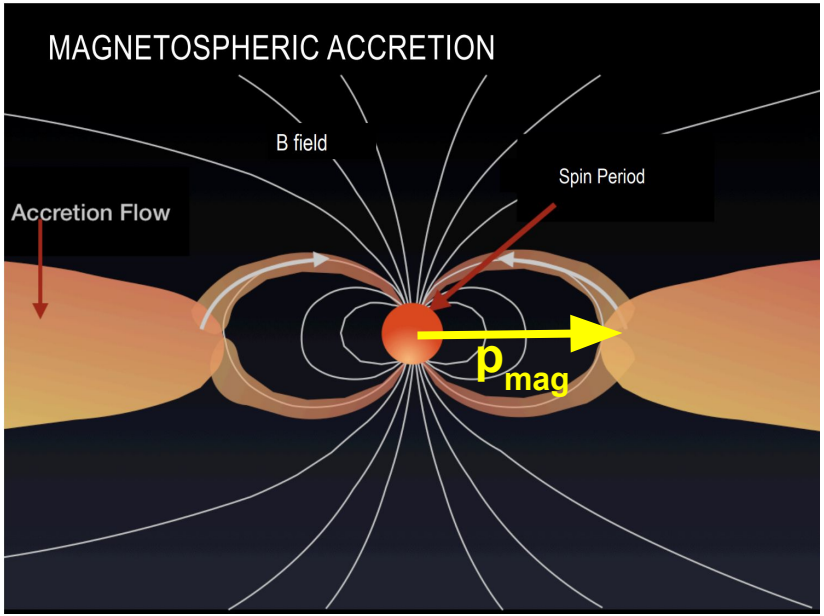

Disk truncation via magnetic pressure

Fig from
https://meetings.iac.es/NS-EWASS-2015/talks/461dangelo_S11.pdf

The Constraint : Position of Magnetosphere

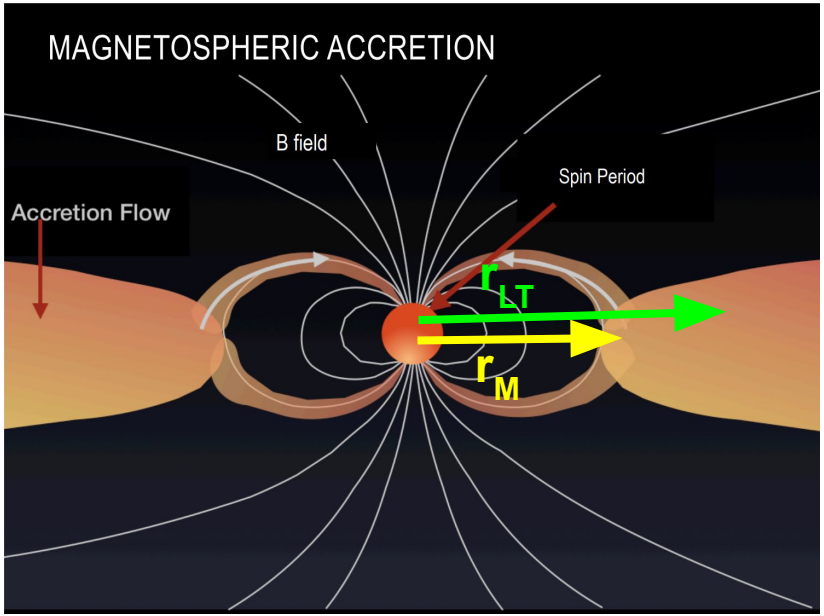

$$r_{\rm LT} >> r_{\rm M} = \eta \left(\frac{\mu^4}{GM\dot{M}^2} \right)^{2/7}$$

(Čemeljić, Kluźniak, Kundu 25)

Fig from
https://meetings.iac.es/NS-EWASS-2015/talks/461dangelo_S11.pdf

The Constraint : Position of Magnetosphere

Table from Čemeljić, Kluźniak, Kundu 25.

Table 2. PULX Properties

Parameter	ULX-7 M51	M82 X-2	NGC 7793 P13
a_* $[10^{-4}]$	1.3	2.8	9.1
$r_{\rm LT}$ [10 km]	4.6	3.2	3.3

The Constraint : Position of Magnetosphere

Non-beamed models: Magnetic field estimated from spin-up/down rates

Table 2. PULX Properties

Table from Čemeljić, Kluźniak, Kundu 25.

Parameter	ULX-7 M51	M82 X-2	NGC 7793 P13
a_* [10^{-4}]	1.3	2.8	9.1
r_{LT} [10 km]	4.6	3.2	3.3
Non-beamed models			
λ_{Edd}	20	200	50
B [10^{12} G]	0.8–70	>10	5
r_M[10 km]	16-210	36	36

The Constraint : Position of Magnetosphere

Non-beamed models: Magnetic field estimated from spin-up/down rates
Beamed models: King, Lasota, Kluzniak 2017 - magnetospheric accretion + beaming

Table from Čemeljić, Kluźniak, Kundu 25.

Table 2. PULX Properties

Parameter	ULX-7 M51	M82 X-2	NGC 7793 P13
a_* [10^{-4}]	1.3	2.8	9.1
r_{LT} [10 km]	4.6	3.2	3.3
Non-beamed models			
λ_{Edd}	20	200	50
B [10^{12} G]	0.8–70	>10	5
r_M[10 km]	16-210	36	36
Beaming model			
b	0.09	0.06	0.18
λ_{Edd}	1.8	12	9
B [10^{10} G]	0.69–19	10	1
r_M[10 km]	2.1–14	6	2

Notes. The radial distance, r_{LT}, at which the Lense-Thirring precession frequency of the inner disk and torus matches ν_{QPO}, is contrasted with the magnetospheric radius, r_M, in both beaming and non-beamed models of the three PULXs. General-relativistic precession modes can exist only when $r_{LT} > r_M$.

The Constraint : Position of Magnetosphere

Non-beamed models: Magnetic field estimated from spin-up/down rates

Beamed models: King, Lasota, Kluzniak 2017 - magnetospheric accretion + beaming

Table from Čemeljić, Kluźniak, Kundu 25.

Table 2. PULX Properties

Parameter	ULX-7 M51	M82 X-2	NGC 7793 P13
a_* [10^{-4}]	1.3	2.8	9.1
r_{LT} [10 km]	4.6	3.2	3.3
Non-beamed models			
λ_{Edd}	20	200	50
B [10^{12} G]	0.8–70	>10	5
r_M[10 km]	16-210	36	36
Beaming model			
b	0.09	0.06	0.18
λ_{Edd}	1.8	12	9
B [10^{10} G]	0.69–19	10	1
r_M[10 km]	2.1–14	6	2

Notes. The radial distance, r_{LT}, at which the Lense-Thirring precession frequency of the inner disk and torus matches ν_{QPO}, is contrasted with the magnetospheric radius, r_M, in both beaming and non-beamed models of the three PULXs. General-relativistic precession modes can exist only when $r_{LT} > r_M$.

LT model excluded in most cases

Case 2. The Magnetic Precession Model

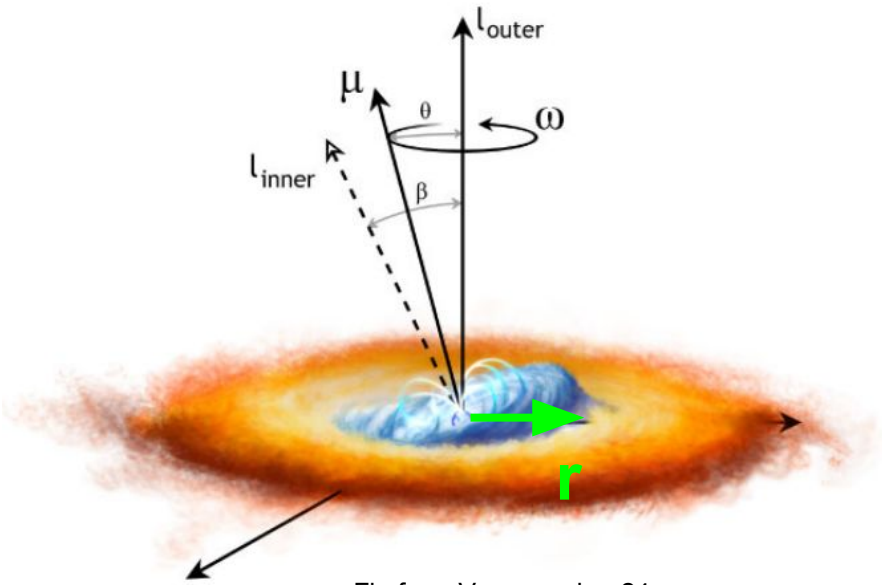

Fig from Veresvarska+24

Formula from Lai 99,
verified numerically by Pfeiffer+04

$$\nu(r) = \frac{\mu^2}{2\pi^3 r^7 \Omega(r)\Sigma(r)D(r)} F(\theta)$$

μ : magnetic moment

Ω : keplerian frequency

Σ : column density

D : a measure of disk thickness

F : magnetic disk threading

Assumptions

$$\nu(r) = \frac{\mu^2}{2\pi^3 r^7 \Omega(r) \Sigma(r) D(r)} F(\theta)$$

1. No threading of the disk by stellar field at the inner edge.

Assumptions

$$\nu(r) = \frac{\mu^2}{2\pi^3 r^7 \Omega(r)\Sigma(r)D(r)} F(\theta)$$

1. No threading of the disk by stellar field at the inner edge.

Figs from Čemeljić19.

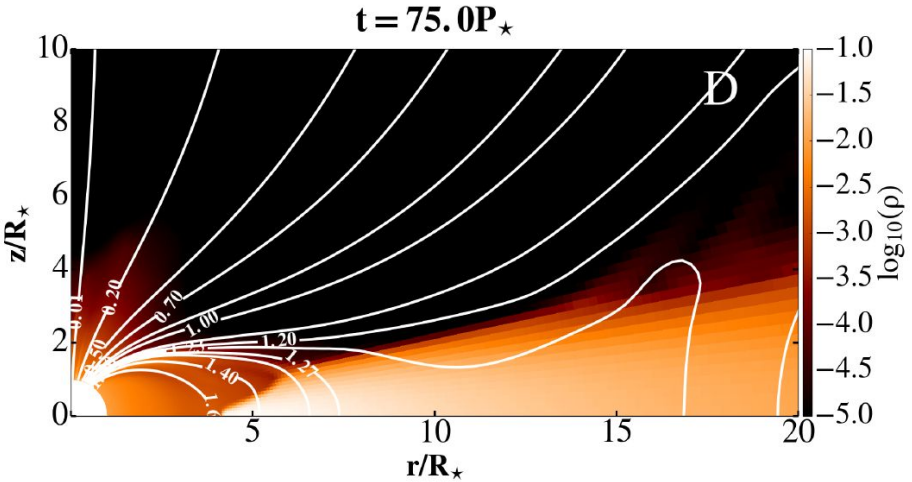

Threading

Assumptions

$$\nu(r) = \frac{\mu^2}{2\pi^3 r^7 \Omega(r)\Sigma(r)D(r)} F(\theta)$$

1. No threading of the disk by stellar field at the inner edge.

Figs from Čemeljić19.

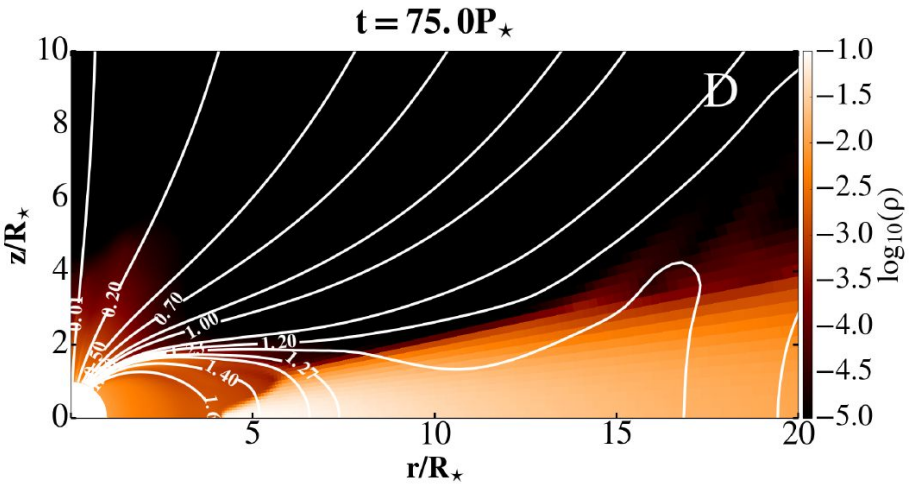

Threading

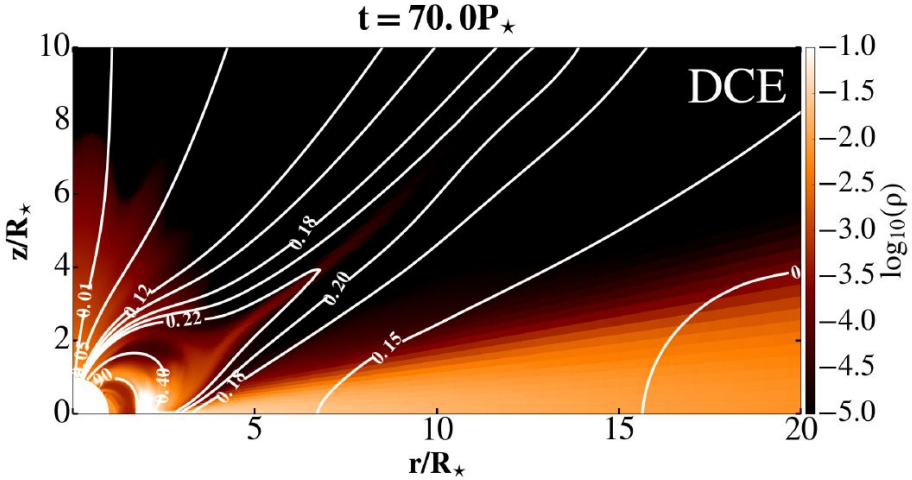

No-threading

Assumptions

$$\nu(r) = \frac{\mu^2}{2\pi^3 r^7 \Omega(r)\Sigma(r)D(r)} F(\theta)$$

1. No threading of the disk by stellar field at the inner edge.

Figs from Čemeljić19.

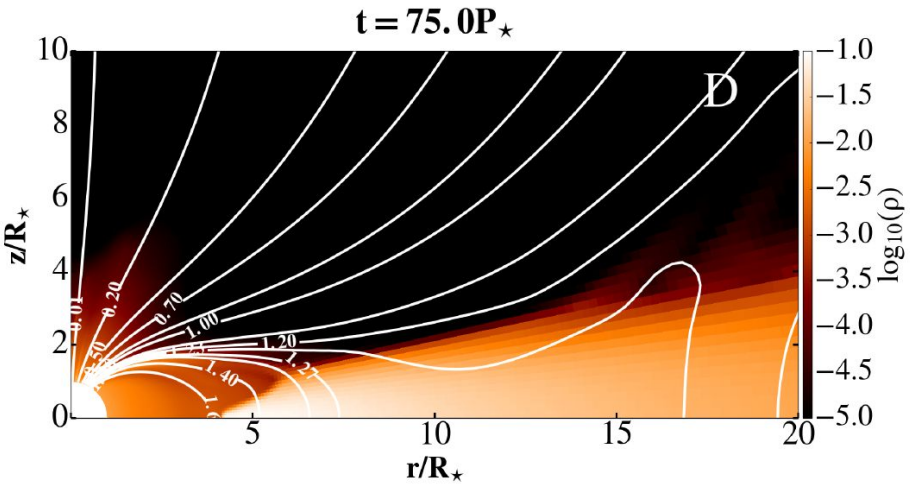

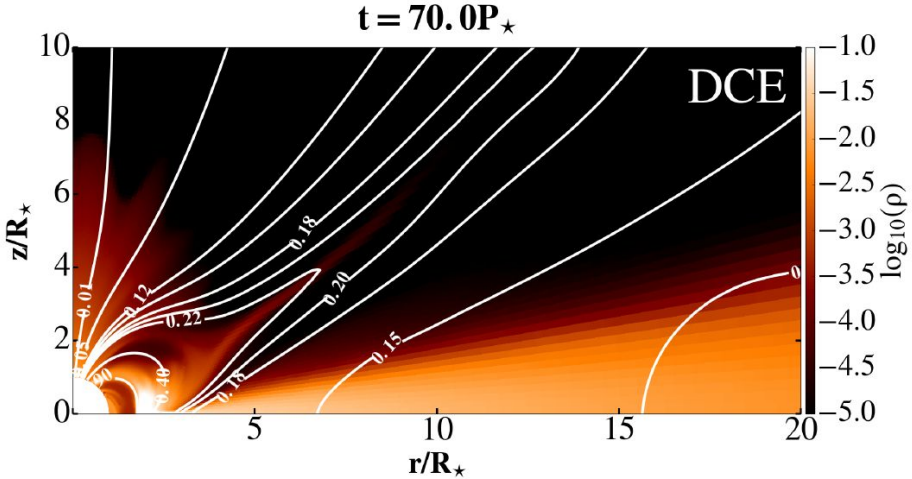

Threading $f \approx 0$ **No-threading** $f \approx 1$

$$F(\theta) = 2f cos^2(\theta) - sin^2(\theta), f \approx 1$$

Assumptions

$$\nu(r) = \frac{\mu^2}{2\pi^3 r^7 \Omega(r) \Sigma(r)}$$

2. The Geometric factor to be close to unity.

$$D = \sqrt{2H/r} \approx 1$$

Geometrically Thick Inner Disk

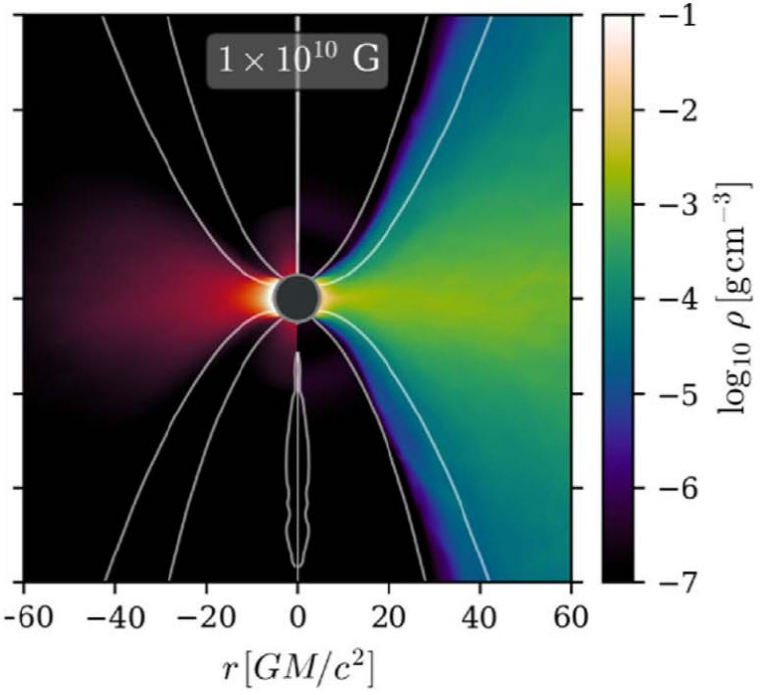

Fig from Kayanikhoo+25.

Assumptions

$$\nu(r) = K' \frac{\mu^2}{\pi^2 r^5 \dot{M}}$$

2. The Geometric factor to be close to unity.

$$D = \sqrt{2H/r} \approx 1$$

Geometrically Thick Inner Disk

3. Radial velocity proportional to azimuthal velocity : in both thin/thick disk

$$v_r = -K' r \Omega$$

$$\dot{M} = -2\pi r v_r \Sigma$$

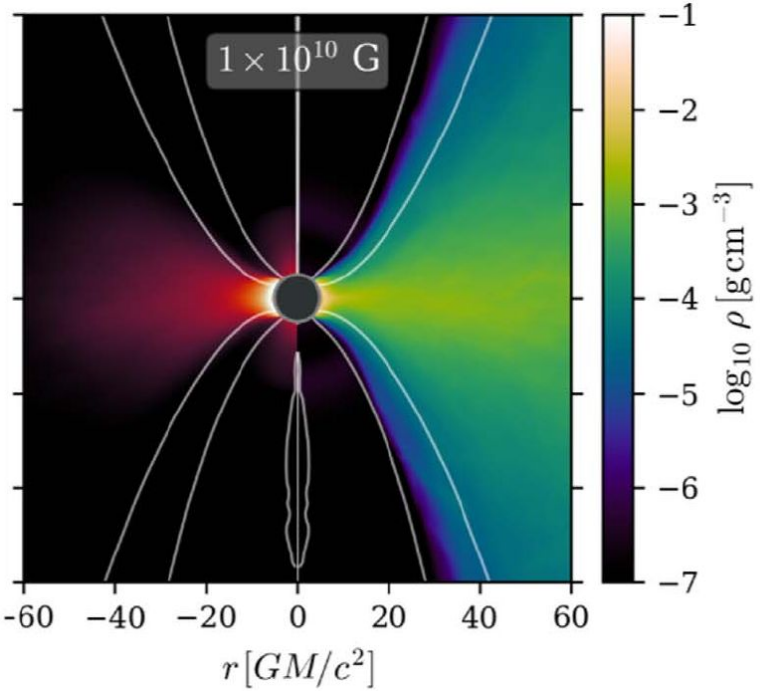

Fig from Kayanikhoo+25

Assumptions

$$\nu(r) = K' \frac{\mu^2}{\pi^2 r^5 \dot{M}}$$

4. Disk magnetically truncated below co-rotation radius.

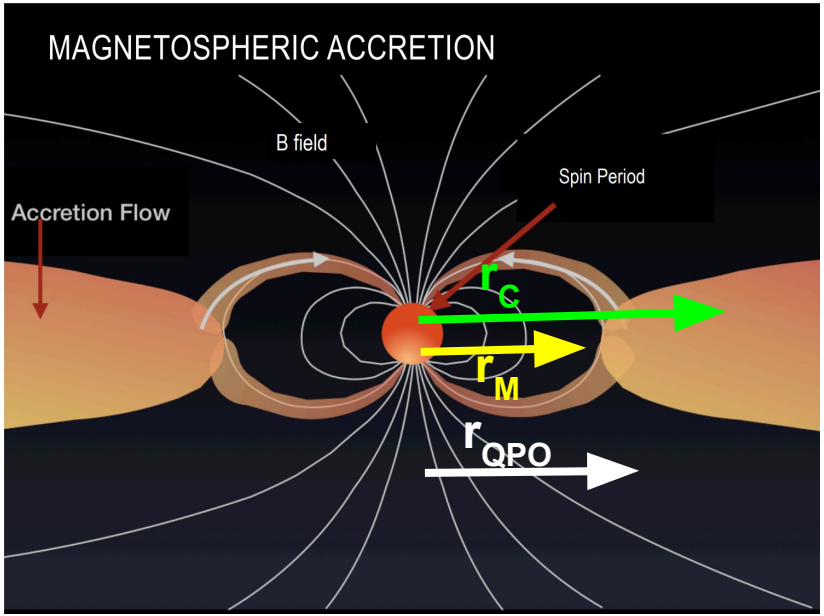

$$r/d = R_{\rm in} = \tilde{\eta} \left(\frac{GMP^2}{4\pi^2} \right)^{1/3} = \eta \left(\frac{\mu^4}{GM\dot{M}^2} \right)^{1/7}$$

Fig from
https://meetings.iac.es/NS-EWASS-2015/talks/461dangelo_S11.pdf

Result

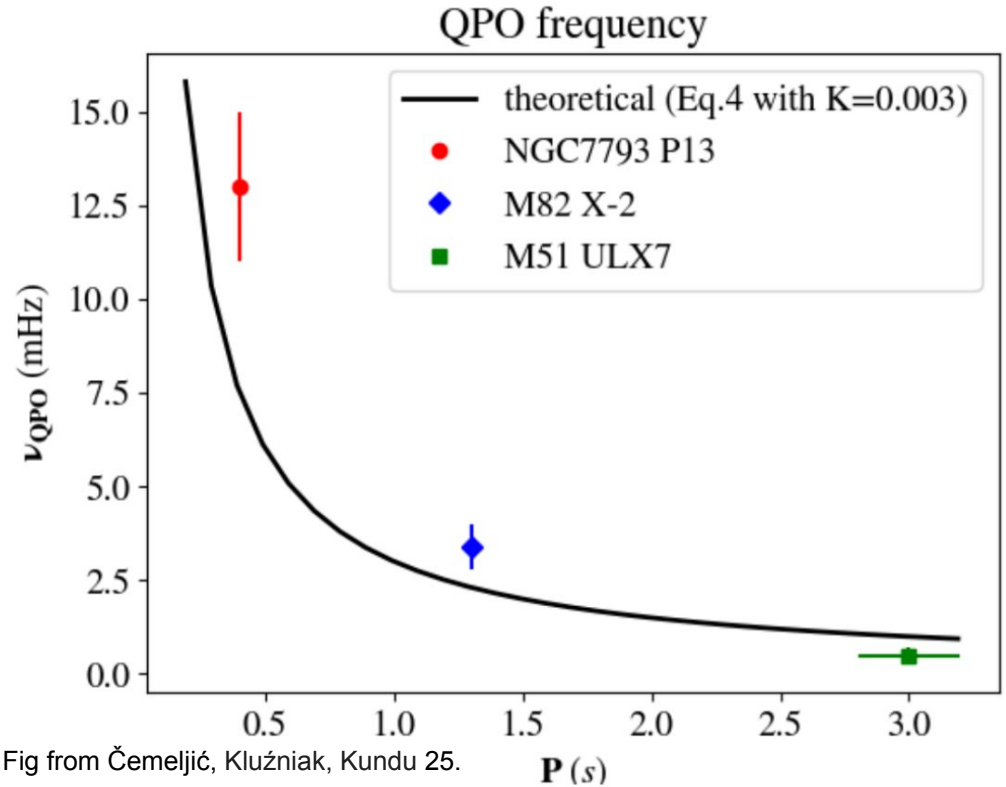

$$\nu = K/P_*$$

Fig from Čemeljić, Kluźniak, Kundu 25.

Conclusions

1. General relativistic frame-dragging is excluded in most cases as a viable model for PULX QPOs.

Conclusions

1. General relativistic frame-dragging is excluded in most cases as a viable model for PULX QPOs.
2. Dong Lai’s magnetic precession acts as a viable alternative for the QPOs.

Conclusions

1. General relativistic frame-dragging is excluded in most cases as a viable model for PULX QPOs.
2. Dong Lai's magnetic precession acts as a viable alternative for the QPOs.
3. The final formula connecting the QPO frequency and spin period has no dependence on magnetic field or accretion rate, making it broadly applicable across sources.

Conclusions

1. General relativistic frame-dragging is excluded in most cases as a viable model for PULX QPOs.
2. Dong Lai's magnetic precession acts as a viable alternative for the QPOs.
3. The final formula connecting the QPO frequency and spin period has no dependence on magnetic field or accretion rate, making it broadly applicable across sources.
4. The QPO frequency is predicted to be around 2-3 orders of magnitude lower than the spin frequency, supported by observations.

Conclusions

1. General relativistic frame-dragging is excluded in most cases as a viable model for PULX QPOs.
2. Dong Lai's magnetic precession acts as a viable alternative for the QPOs.
3. The final formula connecting the QPO frequency and spin period has no dependence on magnetic field or accretion rate, making it broadly applicable across sources.
4. The QPO frequency is predicted to be around 2-3 orders of magnitude lower than the spin frequency, supported by observations.

We await more observations that can help us constrain the geometric factors.